How to cite: *Angew. Chem. Int. Ed.* **2022,** *61,* e202212595
International Edition: doi.org/10.1002/anie.202212595
German Edition: doi.org/10.1002/ange.202212595

Atropisomerism

Ruthenium(II)/Imidazolidine Carboxylic Acid-Catalyzed C–H Alkylation for Central and Axial Double Enantio-Induction

*Yanjun Li, Yan-Cheng Liou, João C. A. Oliveira, and Lutz Ackermann**

Abstract: Enantioselective C–H activation has surfaced as a transformative toolbox for the efficient assembly of chiral molecules. However, despite of major advances in rhodium and palladium catalysis, ruthenium(II)-catalyzed enantioselective C–H activation has thus far largely proven elusive. In contrast, we herein report on a ruthenium(II)-catalyzed highly regio-, diastereo- and enantioselective C–H alkylation. The key to success was represented by the identification of novel C2-symmetric chiral imidazolidine carboxylic acids (CICAs), which are easily accessible in a one-pot fashion, as highly effective chiral ligands. This ruthenium/CICA system enabled the efficient installation of central and axial chirality, and featured excellent branched to linear ratios with generally $>20:1$ dr and up to $98:2$ er. Mechanistic studies by experiment and computation were carried out to understand the catalyst mode of action.

Introduction

In recent years, ruthenium(II)-catalyzed C–H activation has emerged as an increasingly-powerful strategy for efficient molecular synthesis.[1,2] Thus, seminal contributions on ruthenium(II)-catalyzed C–H transformations by Oi and Inoue,[2f] Ackermann,[2d] as well as Bruneau and Dixneuf,[1a] demonstrated its distinct reactivity and selectivity. Despite these indisputable advances, full selectivity control for ruthenium(II)-catalyzed enantioselective C–H activations continues to be underdeveloped,[3–10] with to date only a few examples being described. Hence, Cui[4] and Wang[5] developed ruthenium(II)-catalyzed enantioselective intramolecular C–H activation/hydroarylation through the use of a chiral transient directing group (cTDG) albeit only in an intramolecular fashion (Scheme 1A). As an alternative, the combination of chiral carboxylic acids (CCAs) with transition metals has emerged as a powerful platform for enantioselective C–H activations. Key insights by Reutov on palladium-mediated stereoselective C–H activation were followed by subsequent studies by Yu.[11] In contrast, group 9 transition metals (TM = cobalt,[12] rhodium,[13] iridium[14]) were devised for enantioselective C–H activations by among others Ackermann, Cramer, Matsunaga, Shi, and He. In this context, the use of chiral imidazolidine carboxylic acids (CICAs) in ruthenium catalysis was also disclosed by our group, thus achieving an enantioselective intramolecular hydroarylation.[7] Subsequently, Shi[8] and Matsunaga[9] realized ruthenium(II)-catalyzed enantioselective C–H activation/annulation of sulfoximines using chiral binaphthyl monocarboxylic acids. Therefore, the design and exploration of novel CCAs to overcome the major existing challenges of ruthenium(II)-catalyzed intermolecular enantioselective C–H transformations is highly desired.

Axially chiral molecules have been recognized as ubiquitous structural motifs in biologically-active natural products, chiral recognition reagents, and material sciences.[15] Transition metal-catalyzed enantioselective C–H functionalizations provided a versatile platform to establish axial chirality.[15–17] However, these catalysis systems have largely relied on cost-intensive palladium, rhodium, and iridium catalysts.[17] In addition, these studies focused on the preparation of atropisomers with a single stereogenic element. In contrast, the simultaneous installation of central and axial chirality continues to be rare, owing to the significant challenges in assembling multiple chiral elements with high diastereo-, and enantiocontrol.[18–22] Cramer elegantly reported the iridium(III)-catalyzed enantioselective C–H activation of phosphine oxides and couplings with diazides to construct phosphorus centered chirality and axial chirality.[18] Likewise, iridium-catalyzed highly regio-, diastereo-, and enantioselective hydroarylation of vinyl ethers or bicycloalkenes, along with efficient construction of central and axial chirality, was developed by Lassaletta.[19] In addition, the chiral rhodium(III)-catalyzed enantioselective [3+2] annulation of arylnitrones with alkynes was disclosed by Li for the synthesis of axially and centrally chiral indenes.[20a] These findings indicated the potential of a single catalytic enantioselective C–H functionalization process for multiple chirality control in the synthesis of more complex chiral molecular scaffolds.

Within our continuous interest in ruthenium(II)-catalyzed C–H activation, we, hence, questioned whether ruthenium(II)-catalyzed enantioselective intermolecular hydroarylation would enable the creation of central and C–N axial chirality in a single step. It is noteworthy that in

[*] Dr. Y. Li, Y.-C. Liou, Dr. J. C. A. Oliveira, Prof. Dr. L. Ackermann
Institut für Organische und Biomolekulare Chemie,
Georg-August-Universität Göttingen
Tammanstraße 2, 37077, Göttingen (Germany)
E-mail: Lutz.Ackermann@chemie.uni-goettingen.de

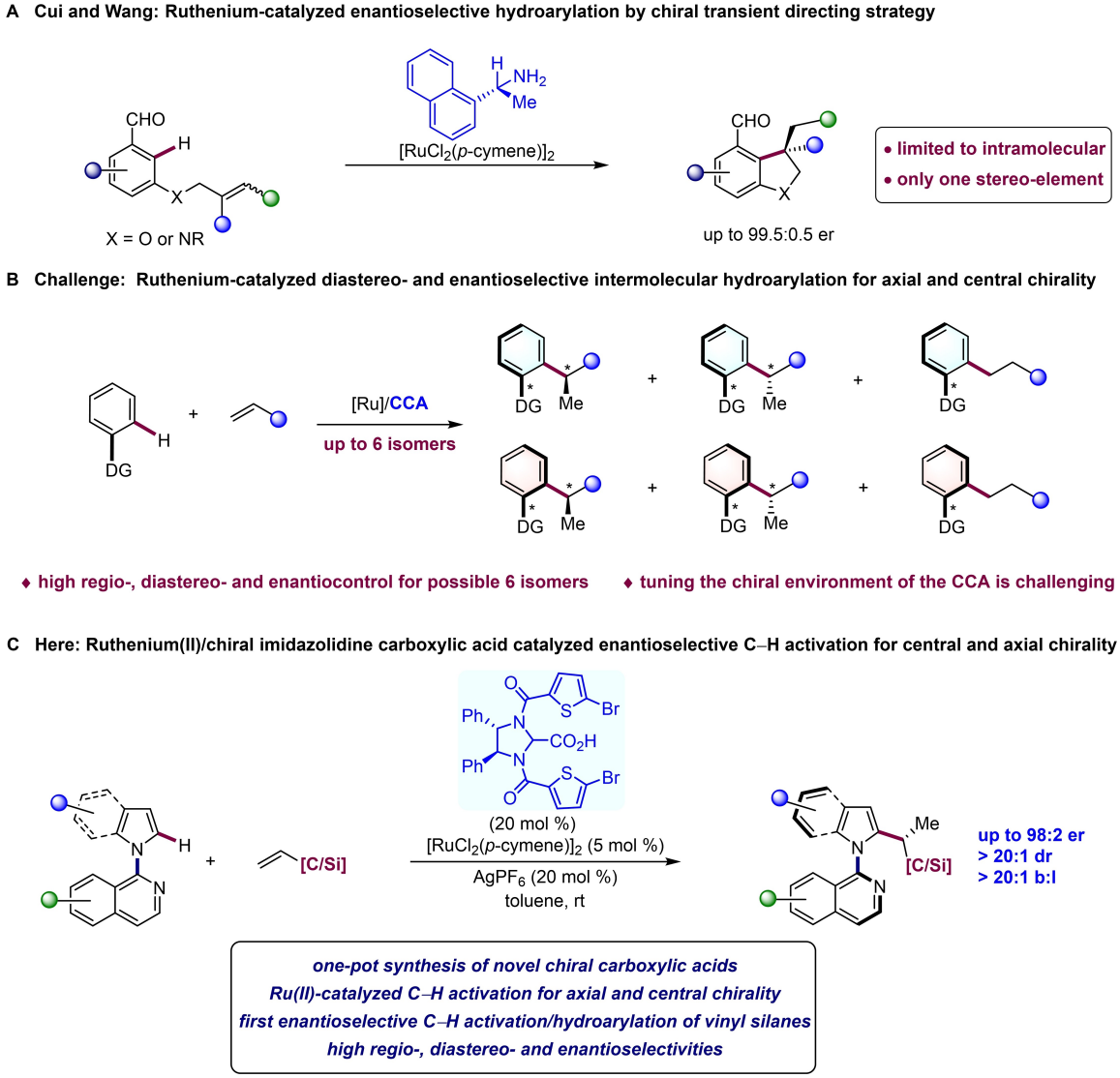

Scheme 1. Ruthenium(II)-catalyzed enantioselective C–H activation/hydroarylation.

comparison with axially chiral C–C atropisomers, C–N atropoisomers are considerably more difficult to realize due to the relatively lower rotational barriers.[23] Owing to the formidable challenges associated with the exact tuning of the chiral environment of CCAs for regio-, diastereo- and enantio-selectivity for possible 6 isomers, this transformation has not been reported to date (Scheme 1B). As a consequence, we became interested in the design of novel CCAs and exploring ruthenium-catalysis systems to overcome these formidable challenges.[24] As a result of our studies, we have now identified a ruthenium(II)-catalyzed diastereo- and enantio-selective C–H functionalization enabled by a CICA ligand (Scheme 1C), on which we report herein. Salient features of our findings include (a) ruthenium(II)-catalyzed enantioselective C–H activation for axial and central chirality, (b) the first enantioselective C–H activation/hydroarylation of vinyl silanes, (c) a one-pot synthesis of novel chiral carboxylic acids, and (d) key mechanistic insights by experiment and computation.

Results and Discussion

Optimization of the Reaction Conditions

We first chose *N*-isoquinoline indole **1** and allylbenzene **2** as the model substrates for the envisioned ruthenium(II)-catalyzed twofold-enantioselective C–H activation (Scheme 2 and Table S1 in the Supporting Information). With $[RuCl_2(p\text{-cymene})]_2$ as the catalyst and $AgSbF_6$ as the additive in toluene at ambient temperature, the impact of various chiral acids was probed. Initially, C2-symmetrical chiral imidazolidine carboxylic acid (CICA) **L1** was tested. **L1** selectively provided the branched product **3** in 63 % yield with promising enantioselectivity of 85.5:14.5 er. Therefore, we set out to prepare novel CICAs. The new CICAs **L5** and **L6** with thiophene-2-carbonyl imidazolidine scaffolds proved optimal, leading to a high enantiocontrol of up to 94.5:5.5 er. The use of $AgPF_6$ as additive resulted in a slightly improved enantioselectivity (95.5:4.5 er). In sharp

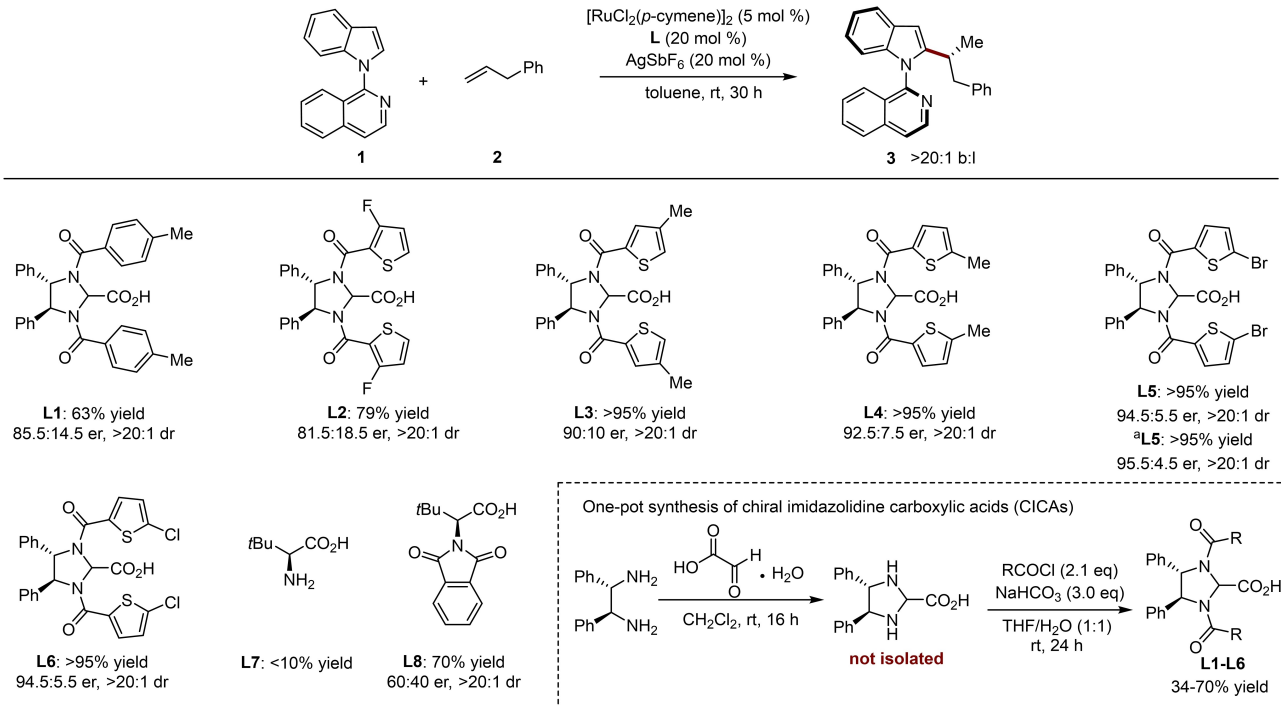

Scheme 2. Optimization of ruthenium(II)-catalyzed enantioselective C–H functionalization. Reaction conditions: **1** (0.10 mmol), **2** (0.30 mmol), $[RuCl_2(p\text{-cymene})]_2$ (5 mol%), ligand (20 mol%), $AgSbF_6$ (20 mol%), toluene (1.0 mL), room temperature (23 °C). Yield and b:l values were determined by ^1H NMR. The er value was determined by HPLC analysis. b:l is the ratio of branched/linear product. [a] $AgPF_6$ (20 mol%) as additive.

contrast, amino acid **L7** as chiral ligand led to significantly lower yield. *N*-protected amino acid **L8** afforded product **3** in good yield, but with poor enantioselectivity (60:40 er). It is worth noting that the novel CICA ligands were easily accessible in a one-pot fashion from chiral diphenylethylenediamine.

Substrate Scope

With the optimized novel ligands in hand, we next explored their generality in the ruthenium(II)-catalyzed enantioselective C–H alkylation (Scheme 3). A broad range of indoles proved compatible, with high elements of enantioselectivities (94:6–98:2 er) and excellent diastereoselectivities (> 20:1 dr) (Scheme 3A). Various electrophilic functional groups, including methoxyl, methyl, ester, trifluoromethyl, nitro, fluoro, chloro and bromo, were well tolerated, affording the products **4**–**12** with high yields, enantioselectivity and diastereoselectivity. Next, we probed the effect of substituents on the isoquinoline (Scheme 3B). The halogen-functional groups in different positions did not significantly affect the diastereoselectivity or enantioselectivity (**15**–**18**). Noteworthily, nitro-substituted isoquinoline also gave the corresponding product **19** in good yield and high er. Subsequently, we explored the viable scope of alkenes (Scheme 3C). Allyl arenes with different functionalities, such as bromo (**20**, **33**), fluoro (**21**), methoxyl (**22**), chloro (**24**–**25**), naphthyl (**23**), trifluoromethyl (**27**), trifluoromethoxy (**28**), ethoxycarbonyl (**29**), were well compatible. The reaction of pyrroles proceeded efficiently to give the alkylated products **31**–**32** with excellent diastereoselectivities, albeit with slightly reduced enantioselectivities. The absolute configuration of product **33** was unambiguously verified by single-crystal X-ray diffraction analysis (CCDC 2165781), featuring a (R_a,*R*)-configuration.[25] Non-activated alkyl-substituted alkenes were also identified as feasible substrates, generating products **34**–**35**. However, lower enantioselectivities were obtained as compared to allylbenzene derivatives. These results imply that the π-chelating interaction between the CICA ligand and alkenes may play a pivotal role for the enantiocontrol. The ruthenium(II)-catalyzed hydroarylation showed a good tolerance to diverse functional groups and provided an attractive strategy for the facile modification of natural products or drug molecules. Allyl arenes **S36**–**S37** derived from Gemfibrozil and Estrone were subjected to the reaction, affording the products **36**–**37** in good yields with high stereoselectivities, respectively. Moreover, gaseous alkenes were also suitable partners for this transformation. Hence, ethylene provided the desired ethylated product **38** in 66% yield with 65:35 er. Likewise, propylene afforded the isopropylated products **39**–**40** with an enantioselectivities of 84:16 er.

Chiral organosilanes represent key structural motifs in numerous natural products and drug candidates.[26] However, only a limited number of methods for the catalytic enantioselective synthesis of chiral silanes is thus far available.[26c] Hence, we wondered whether our ruthenium(II)/CICAs system would be suitable for the challenging hydroarylation of vinyl silanes to prepare chiral organo-

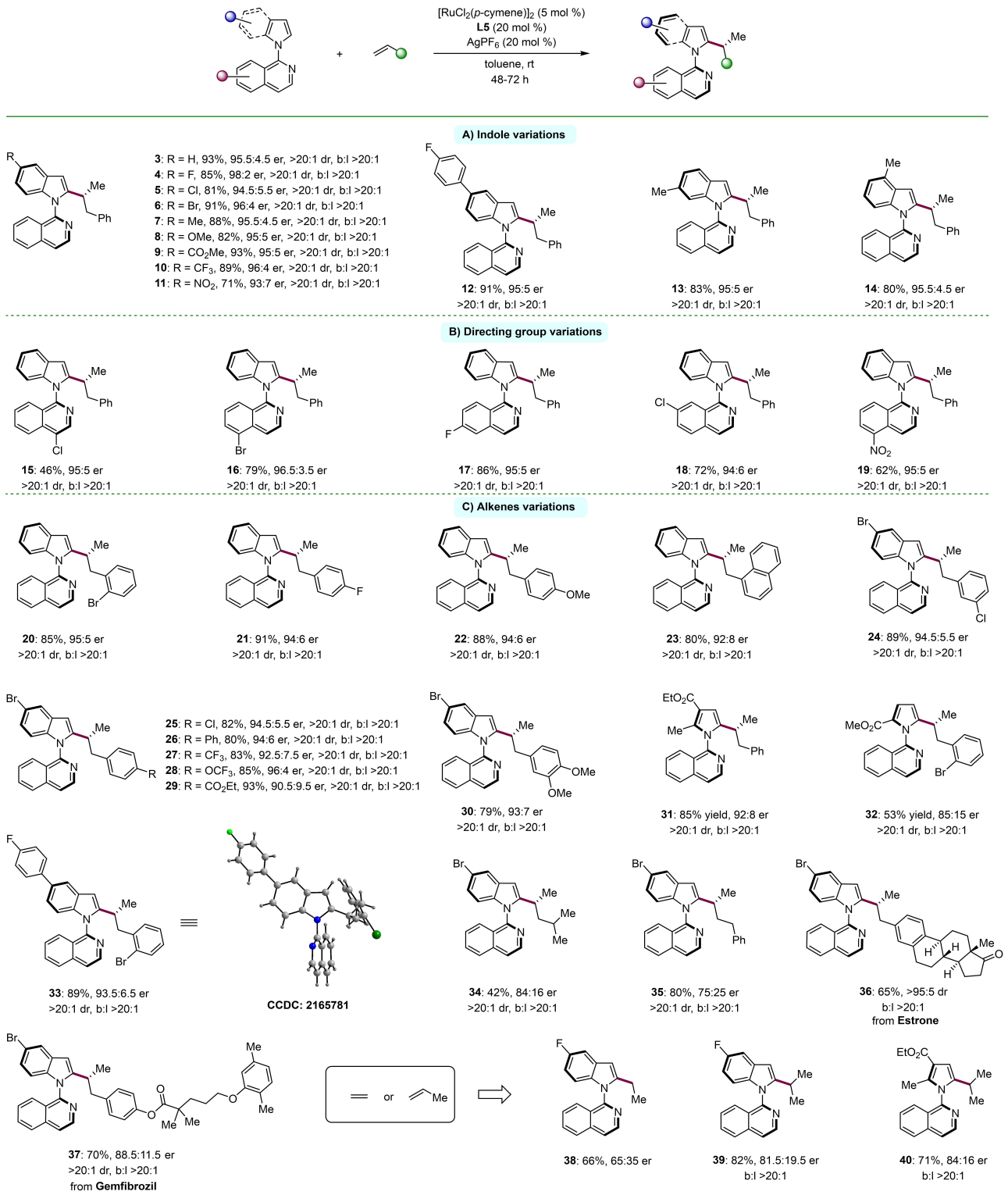

Scheme 3. Scope of ruthenium(II)-catalyzed enantioselective C–H functionalization.

silanes (Scheme 4). To our delight, these transformations exhibited excellent diastereo- and enantio-selectivities. Triarylvinylsilanes bearing various electron-donating groups (Me, *t*Bu, or OMe) or inductively electron-withdrawing group (Cl) were coupled with indoles/pyrroles, yielding the desired products (**41**–**51**) in good yields with up to 97.5:2.5 er and >20:1 dr. The reaction of vinyl trimethyl silane gave the product **52** with excellent diastereoselectivity, albeit with somewhat reduced enantioselectivity. To the best of our knowledge, these are the first examples of

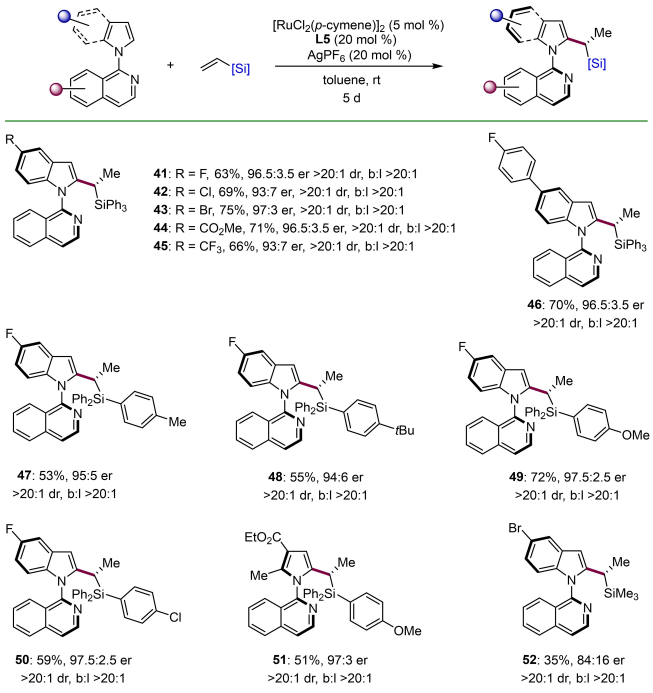

Scheme 4. Scope of vinyl silanes.

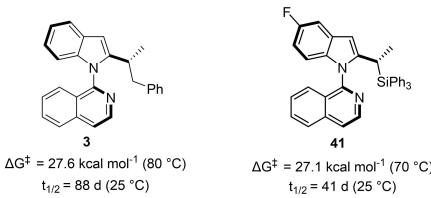

Scheme 5. Experimental determination of the rotational barrier and half-life for epimerization of **3** and **41**.

enantioselective C–H activation/hydroarylation of vinyl silanes.

The stereochemical stabilities of the axially chiral products were evaluated using experimental methods (Scheme 5). First, no diminished diastereoselectivities of the products were observed after their storage in a freezer for a several months. Second, we determined the rotational barriers of the representative compounds **3** and **41** in toluene-d_8 at 70 or 80 °C. The rotational barriers and half-life for epimerization of **3** and **41** are summarized in Scheme 5.

Mechanistic Studies

In order to shed light on the operative catalysis of the ruthenium(II)-catalyzed enantioselective C–H functionalization, the kinetic isotope effect (KIE) experiment was performed by parallel reactions of substrates **1**D and **1** with **2** (Scheme 6A). The KIE of $k_H/k_D \approx 1.3$ was indicative of the C–H scission not being involved in the rate-determining step. Next, the catalytic hydroarylation of **1** was performed

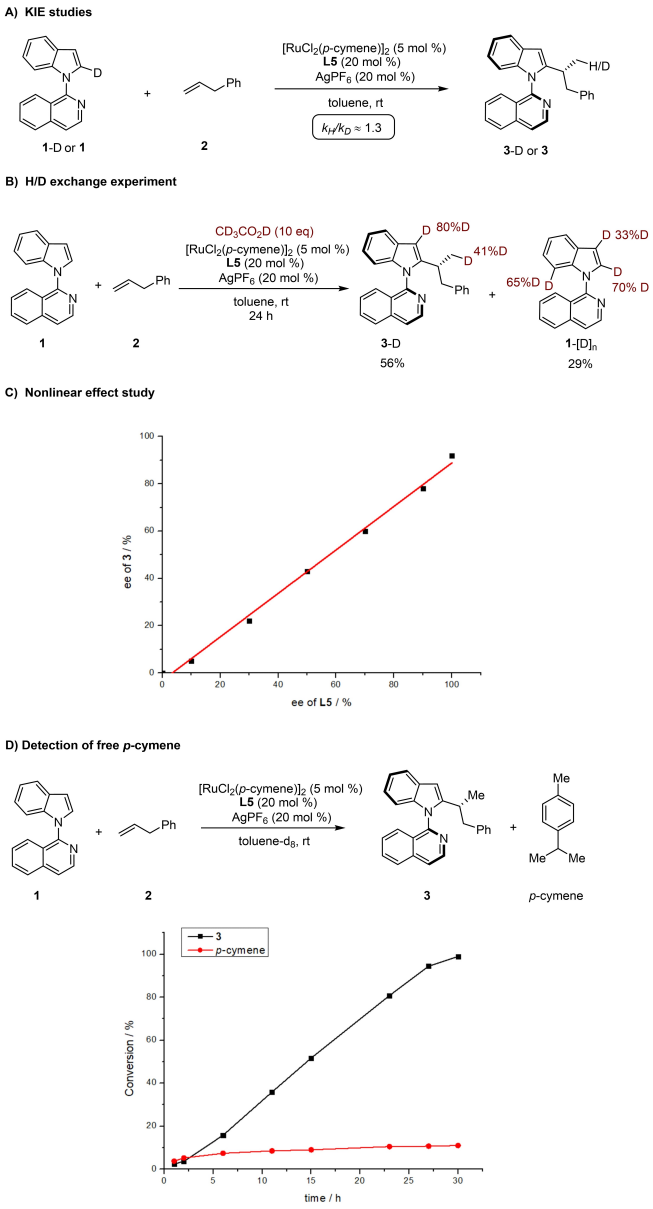

Scheme 6. Key mechanistic Findings.

in the presence of isotopically labeled CD_3CO_2D (Scheme 6B). H/D incorporation was observed at the methyl group of product **2** and H/D exchange occurred in the substrate **1**, which further demonstrate that the C–H activation step is reversible. Furthermore, a linear correlation was observed by nonlinear-effect (NLE) studies on the enantiomeric composition of chiral acid **L5** and **3** (Scheme 6C). Monitoring the reaction by ^{1}H NMR showed that only about 10 % of free *p*-cymene (based on $[RuCl_2(p\text{-cymene})]_2$) were released during the entire period of the reaction (Scheme 6D), implying the (*p*-cymene)ruthenium(II) species being the key intermediates.

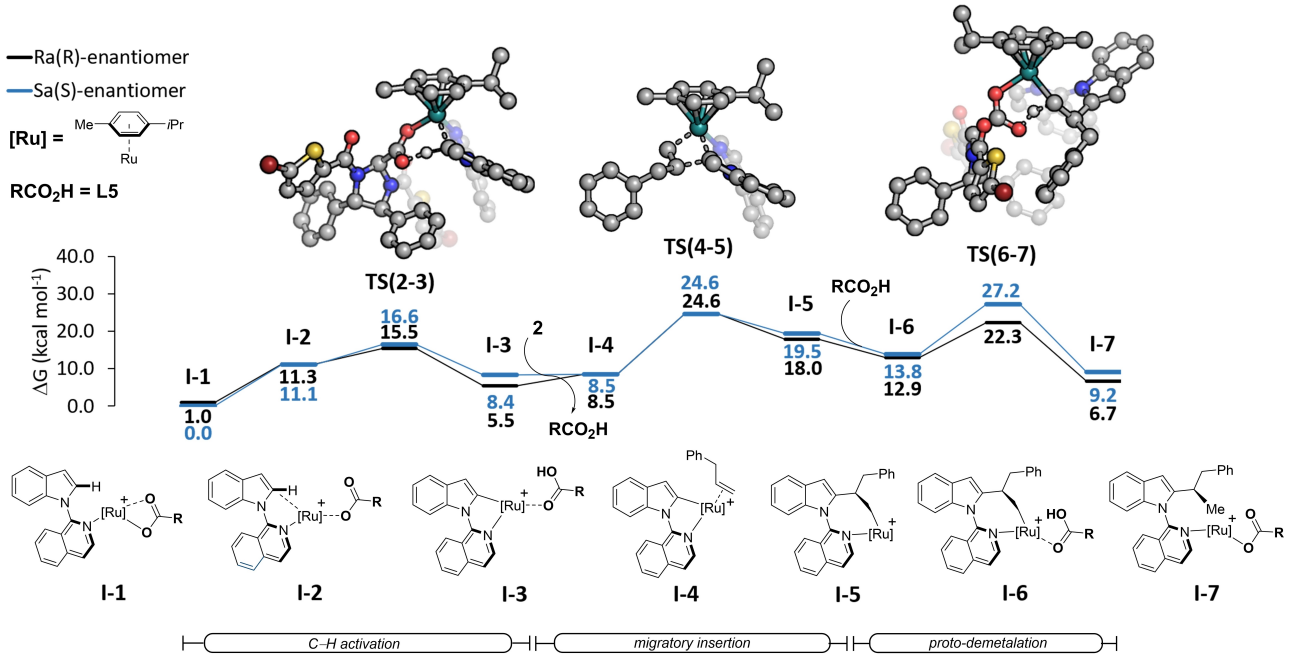

Figure 1. Computed relative Gibbs free energies ($\Delta G_{298.15\,K}$) in kcal mol^{-1} between the C–H activation and proto-demetalation elementary steps at the PW6B95-D4/def2-TZVPP-SMD(toluene)//PBE0-D3BJ/def2-SVP level of theory for both enantiomers. [Ru] = Ru(*p*-cymene), and RCO_2H = **L5**. For clarity only the structures for the preferred pathway are shown. In the transition state structures non-relevant hydrogens were omitted.

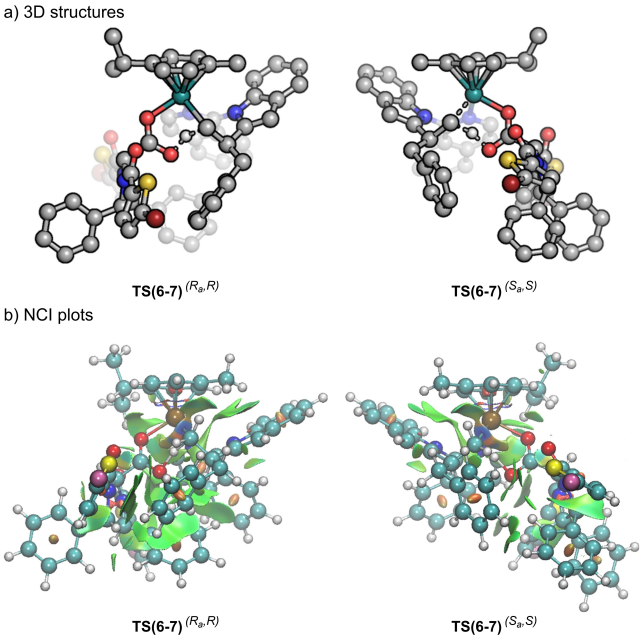

Figure 2. a) 3D structures for the transition states involved in the proto-demetalation step for both (R_a,R)- and (S_a,S)-enantiomers. b) respective visualisation of the non-covalent interactions calculated with the help of the NCIPLOT program. In the plotted surfaces, red corresponds to strong repulsive interactions, while green and blue correspond to weak and strong interactions, respectively.

Computational Studies

Subsequently the catalyst mode of action, was assessed by means of DFT calculations carried out at the PW6B95-D4/def2-TZVPP-SMD(toluene)//PBE0-D3BJ/def2-SVP level of theory, between the C–H activation and the proto-demetalation elementary steps (Figure 1).[27] These studies explained the two most energetically favourable pathways for the (R_a,R)- and (S_a,S)-enantiomers. C–H activation were found to be facile for both enantiomers with the (R_a)-atropoenantiomer transition state **TS(2–3)** being energetically favoured over the (S_a)-atropoenantiomer by 2.1 kcal mol^{-1}, being in good agreement with the experimental studies (Scheme 5A). Interestingly, the axial chirality seems to be already imposed in intermediate **I-1**. Migratory insertion for the (R_a,R)-atropoenantiomer proceeds through **TS(4–5)** with a barrier of 23.6 kcal mol^{-1}, whereas for the (S_a,S)-atropoenantiomer this transition state is destabilized by 1.0 kcal mol^{-1}. Proto-demetalation proceeds upon the coordination of the CICA **L5** through **TS(6–7)** favouring the (R_a,R)-atropoenantiomer over the (S_a,S)-atropoenantiomer pathway by 5.9 kcal mol^{-1}. This stabilization largely results from weak attractive non-covalent interactions between the phenyl moiety prevenient from allylbenzene and the pocket defined by the side-chain and the phenyl backbone moiety of the CICA, which are absent in the **TS(6–7)** for (S_a,S)-atropoenantiomer (Figure 2). The assessment of the energy

profiles point at a difference in the rate-determining step from migratory insertion to proto-demetalation for the (R_a,R)- versus the (S_a,S)-atropoenantiomer. In order to evaluate the effect of dispersion forces in the catalyst mode of action the same studies were conducted in the absence of dispersion corrections (Figure S6), demonstrating that dispersion forces present a relevant role in the migratory insertion and proto-demetalation steps, being crucial in the stabilization of the later.

Proposed Catalytic Cycle

Based on our detailed experimental and computational findings, a plausible catalytic cycle is depicted in Scheme 7. Initially, $[RuCl_2(p\text{-cymene})]_2$ reacts with $AgPF_6$ and CICA **L5** to generate CICA coordinated cationic ruthenium complex **A**. Then, ruthenium species **B** is generated by carboxylate-assisted C–H bond cleavage. Upon alkene coordination, transition state **C** involving non-covalent interactions between the allylbenzene and thiophene of **L5** is proposed. The ligand-assisted migratory insertion into the ruthenium-carbon bond proceeds next to form intermediate **D**. Finally, intermediate **D** undergoes proto-demetalation with CICA **L5** to deliver the desired product **3**.

Conclusion

In summary, we have reported on a highly chemo-, regio-, diastereo- and enantioselective ruthenium(II)-catalyzed C–H alkylation. The design and synthesis of novel C2-symmetric chiral imidazolidine carboxylic acids was the key for outstanding levels of efficiency and selectivity. A broad range of terminal alkenes, including functionalized allyl arenes, simple olefins as well as even gaseous propylene and ethylene, were efficiently converted, constructing central and axial chirality in a single catalytic process. Moreover, chiral organosilanes were thereby accessed with high levels of enantioselectivities and diastereoselectivities. Experimental and computational studies provided strong support for a reversible C–H activation with migratory insertion being the rate-determining step for the major (R_a, R)-enantiomer.

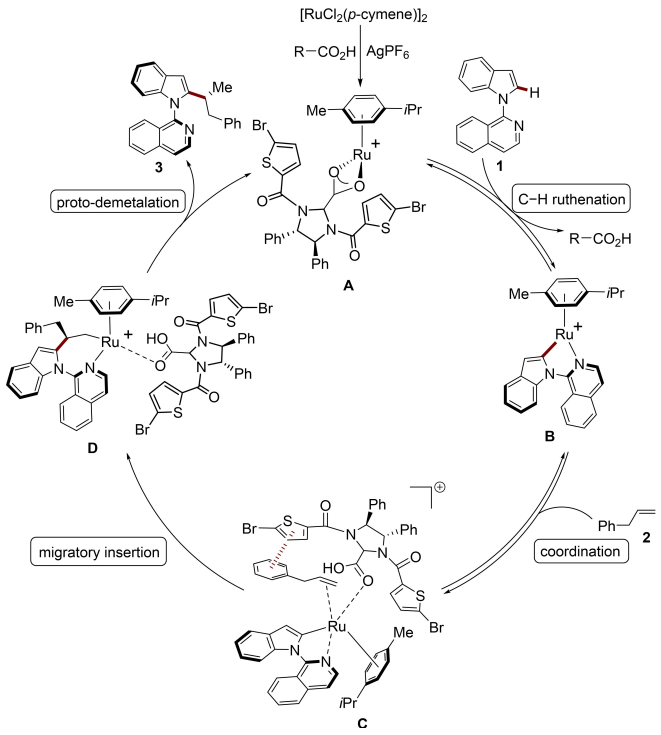

Scheme 7. Proposed catalytic cycle.

Acknowledgements

The authors gratefully acknowledge support from the ERC Advanced Grant no. 101021358, the DFG Gottfried-WilhelmLeibniz award (L. A.). The authors thank Dr. Christopher Golz (University of Göttingen) for the assistance with the X-ray diffraction analysis. Open Access funding enabled and organized by Projekt DEAL.

Conflict of Interest

The authors declare no conflict of interest.

Data Availability Statement

The data that support the findings of this study are available in the supplementary material of this article.

Keywords: Axial Chirality · Central Chirality · Chiral Carboxylic Acid · Enantioselective C–H Activation · Ruthenium

[1] a) P. B. Arockiam, C. Bruneau, P. H. Dixneuf, *Chem. Rev.* **2012**, *112*, 5879–5918; b) L. Ackermann, R. Vicente, *Top. Curr. Chem.* **2009**, *292*, 211–229.

[2] a) C. Shan, L. Zhu, L.-B. Qu, R. Bai, Y. Lan, *Chem. Soc. Rev.* **2018**, *47*, 7552–7576; b) P. Nareddy, F. Jordan, M. Szostak, *ACS Catal.* **2017**, *7*, 5721–5745; c) J. A. Leitch, C. G. Frost, *Chem. Soc. Rev.* **2017**, *46*, 7145–7153; d) L. Ackermann, *Acc. Chem. Res.* **2014**, *47*, 281–295; e) L. Ackermann, *Org. Lett.* **2005**, *7*, 3123–3125; f) S. Oi, S. Fukita, N. Hirata, N. Watanuki, S. Miyano, Y. Inoue, *Org. Lett.* **2001**, *3*, 2579–2581.

[3] For references on palladium-, rhodium-, iridium- and 3d transition metals- catalyzed enantioselective C–H activations, see: a) T. Yoshino, S. Matsunaga, *ACS Catal.* **2021**, *11*, 6455–6466; b) T. K. Achar, S. Maiti, S. Jana, D. Maiti, *ACS Catal.* **2020**, *10*, 13748–13793; c) Q. Shao, K. Wu, Z. Zhuang, S. Qian, J.-Q. Yu, *Acc. Chem. Res.* **2020**, *53*, 833–851; d) J. Diesel, N. Cramer, *ACS Catal.* **2019**, *9*, 9164–9177; e) J. Loup, U. Dhawa, F. Pesciaioli, J. Wencel-Delord, L. Ackermann, *Angew. Chem. Int. Ed.* **2019**, *58*, 12803–12818; *Angew. Chem.* **2019**, *131*, 12934–12949; f) T. G. Saint-Denis, R.-Y. Zhu, G. Chen, Q.-F. Wu, J.-Q. Yu, *Science* **2018**, *359*, eaao4798; g) C. G. Newton, S.-G. Wang, C. C. Oliveira, N. Cramer, *Chem. Rev.* **2017**, *117*, 8908–8976.

[4] Z.-Y. Li, H. H. C. Lakmal, X. Qian, Z. Zhu, B. Donnadieu, S. J. McClain, X. Xu, X. Cui, *J. Am. Chem. Soc.* **2019**, *141*, 15730–15736.

[5] G. Li, Q. Liu, L. Vasamsetty, W. Guo, J. Wang, *Angew. Chem. Int. Ed.* **2020**, *59*, 3475–3479; *Angew. Chem.* **2020**, *132*, 3503–3507.

[6] H. Liang, W. Guo, J. Li, J. Jiang, J. Wang, *Angew. Chem. Int. Ed.* **2022**, *61*, e202204926; *Angew. Chem.* **2022**, *134*, e202204926.

[7] U. Dhawa, R. Connon, J. C. A. Oliveira, R. Steinbock, L. Ackermann, *Org. Lett.* **2021**, *23*, 2760–2765.

[8] T. Zhou, P.-F. Qian, J.-Y. Li, Y.-B. Zhou, H.-C. Li, H.-Y. Chen, B.-F. Shi, *J. Am. Chem. Soc.* **2021**, *143*, 6810–6816.

[9] L.-T. Huang, Y. Hirata, Y. Kato, L. Lin, M. Kojima, T. Yoshino, S. Matsunaga, *Synthesis* **2022**, https://doi.org/10.1055/a-1588-0072.

[10] a) C.-X. Ye, X. Shen, S. Chen, E. Meggers, *Nat. Chem.* **2022**, *14*, 566–573; b) T. Miyazawa, T. Suzuki, Y. Kumagai, K. Takizawa, T. Kikuchi, S. Kato, A. Onoda, T. Hayashi, Y. Kamei, F. Kamiyama, M. Anada, M. Kojima, T. Yoshino, S. Matsunaga, *Nat. Catal.* **2020**, *3*, 851–858; c) Q. Xing, C.-M. Chan, Y.-W. Yeung, W.-Y. Yu, *J. Am. Chem. Soc.* **2019**, *141*, 3849–3853; d) Z. Zhou, S. Chen, Y. Hong, E. Winterling, Y. Tan, M. Hemming, K. Harms, K. N. Houk, E. Meggers, *J. Am. Chem. Soc.* **2019**, *141*, 19048–19057.

[11] a) G. Chen, W. Gong, Z. Zhuang, M. S. Andra, Y. Q. Chen, X. Hong, Y. F. Yang, T. Liu, K. N. Houk, J. Q. Yu, *Science* **2016**, *353*, 1023–1027; b) L. Chu, K.-J. Xiao, J.-Q. Yu, *Science* **2014**, *346*, 451–455; c) B.-F. Shi, Y.-H. Zhang, J. K. Lam, D.-H. Wang, J.-Q. Yu, *J. Am. Chem. Soc.* **2010**, *132*, 460–461; d) B.-F. Shi, N. Maugel, Y.-H. Zhang, J.-Q. Yu, *Angew. Chem. Int. Ed.* **2008**, *47*, 4882–4886; *Angew. Chem.* **2008**, *120*, 4960–4964; e) V. I. Sokolov, L. L. Troitskaya, O. A. Reutov, *J. Organomet. Chem.* **1979**, *182*, 537–546; see also:f) T. Saget, N. Cramer, *Angew. Chem. Int. Ed.* **2012**, *51*, 12842–12845; *Angew. Chem.* **2012**, *124*, 13014–13017; g) S. Anas, A. Cordi, H. B. Kagan, *Chem. Commun.* **2011**, *47*, 11483–11485.

[12] a) Y. Hirata, D. Sekine, Y. Kato, M. Kojima, T. Yoshino, L. Lin, S. Matsunaga, *Angew. Chem. Int. Ed.* **2022**, *61*, e2022053; *Angew. Chem.* **2022**, *134*, e2022053; b) S. Fukagawa, Y. Kato, R. Tanaka, M. Kojima, T. Yoshino, S. Matsunaga, *Angew. Chem. Int. Ed.* **2019**, *58*, 1153–1157; *Angew. Chem.* **2019**, *131*, 1165–1169; c) Y.-H. Liu, P.-X. Li, Q.-J. Yao, Z.-Z. Zhang, D.-Y. Huang, M. D. Le, H. Song, L. Liu, B.-F. Shi, *Org. Lett.* **2019**, *21*, 1895–1899; d) D. Sekine, K. Ikeda, S. Fukagawa, M. Kojima, T. Yoshino, S. Matsunaga, *Organometallics* **2019**, *38*, 3921–3926; e) F. Pesciaioli, U. Dhawa, J. C. A. Oliveira, R. Yin, M. John, L. Ackermann, *Angew. Chem. Int. Ed.* **2018**, *57*, 15425–15429; *Angew. Chem.* **2018**, *130*, 15651–15655.

[13] a) L.-T. Huang, S. Fukagawa, M. Kojima, T. Yoshino, S. Matsunaga, *Org. Lett.* **2020**, *22*, 8256–8260; b) S. Fukagawa, M. Kojima, T. Yoshino, S. Matsunaga, *Angew. Chem. Int. Ed.* **2019**, *58*, 18154–18158; *Angew. Chem.* **2019**, *131*, 18322–18326; c) M. Brauns, N. Cramer, *Angew. Chem. Int. Ed.* **2019**, *58*, 8902–8906; *Angew. Chem.* **2019**, *131*, 8994–8998; d) Y. Sun, N. Cramer, *Angew. Chem. Int. Ed.* **2018**, *57*, 15539–15543; *Angew. Chem.* **2018**, *130*, 15765–15769; e) S. Satake, T. Kurihara, K. Nishikawa, T. Mochizuki, M. Hatano, K. Ishihara, T. Yoshino, S. Matsunaga, *Nat. Catal.* **2018**, *1*, 585–591; f) L. Lin, S. Fukagawa, D. Sekine, E. Tomita, T. Yoshino, S. Matsunaga, *Angew. Chem. Int. Ed.* **2018**, *57*, 12048–12052; *Angew. Chem.* **2018**, *130*, 12224–12228; g) M. V. Pham, N. Cramer, *Chem. Eur. J.* **2016**, *22*, 2270–2273.

[14] a) Y. Kato, L. Lin, M. Kojima, T. Yoshino, S. Matsunaga, *ACS Catal.* **2021**, *11*, 4271–4277; b) L. Liu, H. Song, Y.-H. Liu, L.-S. Wu, B.-F. Shi, *ACS Catal.* **2020**, *10*, 7117–7122; c) W. Liu, W. Yang, J. Zhu, Y. Guo, N. Wang, J. Ke, P. Yu, C. He, *ACS Catal.* **2020**, *10*, 7207–7215; d) Y.-S. Jang, M. Dieckmann, N. Cramer, *Angew. Chem. Int. Ed.* **2017**, *56*, 15088–15092; *Angew. Chem.* **2017**, *129*, 15284–15288.

[15] a) J. K. Cheng, S.-H. Xiang, S. Li, L. Ye, B. Tan, *Chem. Rev.* **2021**, *121*, 4805–4902; b) Q. Wang, Q. Gu, S.-L. You, *Angew. Chem. Int. Ed.* **2019**, *58*, 6818–6825; *Angew. Chem.* **2019**, *131*, 6890–6897; c) C. Min, D. Seidel, *Chem. Soc. Rev.* **2017**, *46*, 5889–5902; d) T. Akiyama, K. Mori, *Chem. Rev.* **2015**, *115*, 9277–9306; e) M. P. Carroll, P. J. Guiry, *Chem. Soc. Rev.* **2014**, *43*, 819–833; f) Q.-L. Zhou, *Privileged Chiral Ligands and Catalysts*, Wiley-VCH, Weinheim, Germany, **2011**; g) J. F. Teichert, B. L. Feringa, *Angew. Chem. Int. Ed.* **2010**, *49*, 2486–2528; *Angew. Chem.* **2010**, *122*, 2538–2582; h) J. Clayden, W. J. Moran, P. J. Edwards, S. R. LaPlante, *Angew. Chem. Int. Ed.* **2009**, *48*, 6398–6401; *Angew. Chem.* **2009**, *121*, 6516–6520; i) V. Farina, J. T. Reeves, C. H. Senanayake, J. J. Song, *Chem. Rev.* **2006**, *106*, 2734–2793; j) W. Tang, X. Zhang, *Chem. Rev.* **2003**, *103*, 3029–3070; k) R. Noyori, H. Takaya, *Acc. Chem. Res.* **1990**, *23*, 345–350.

[16] Selected references: a) N. Jacob, Y. Zaid, J. C. A. Oliveira, L. Ackermann, J. Wencel-Delord, *J. Am. Chem. Soc.* **2022**, *144*, 798–806; b) G. Liao, T. Zhang, L. Jin, B.-J. Wang, C.-K. Xu, Y. Lan, Y. Zhao, B.-F. Shi, *Angew. Chem. Int. Ed.* **2022**, *61*, e202115221; *Angew. Chem.* **2022**, *134*, e202115221; c) C.-Q. Pan, S.-Y. Yin, S.-B. Wang, Q. Gu, S.-L. You, *Angew. Chem. Int. Ed.* **2021**, *60*, 15510–15516; *Angew. Chem.* **2021**, *133*, 15638–15644; d) L. Jin, Q.-J. Yao, P.-P. Xie, Y. Li, B.-B. Zhan, Y.-Q. Han, X. Hong, B.-F. Shi, *Chem* **2020**, *6*, 497–511; e) S. Shaaban, H. Li, F. Otte, C. Strohmann, A. P. Antonchick, H. Waldmann, *Org. Lett.* **2020**, *22*, 9199–9202; f) Z.-S. Liu, Y. Hua, Q. Gao, Y. Ma, H. Tang, Y. Shang, H.-G. Cheng, Q. Zhou, *Nat. Catal.* **2020**, *3*, 727–733; g) Q.-H. Nguyen, S.-M. Guo, T. Royal, O. Baudoin, N. Cramer, *J. Am. Chem. Soc.* **2020**, *142*, 2161–2167; h) Q. Wang, W.-W. Zhang, H. Song, J. Wang, C. Zheng, Q. Gu, S.-L. You, *J. Am. Chem. Soc.* **2020**, *142*, 15678–15685; i) Q. Wang, Z.-J. Cai, C.-X. Liu, Q. Gu, S.-L. You, *J. Am. Chem. Soc.* **2019**, *141*, 9504–9510; j) M. Tian, D. Bai, G. Zheng, J. Chang, X. Li, *J. Am. Chem. Soc.* **2019**, *141*, 9527–9532; k) G. C. G. Newton, E. Braconi, J. Kuziola, M. D. Wodrich, N. Cramer, *Angew. Chem. Int. Ed.* **2018**, *57*, 11040–11044; *Angew. Chem.* **2018**, *130*, 11206–11210; l) G. Shan, J. Flegel, H. Li, C. Merten, S. Ziegler, A. P. Antonchick, H. Waldmann, *Angew. Chem. Int. Ed.* **2018**, *57*, 14250–14254; *Angew. Chem.* **2018**, *130*, 14446–14450; m) C. He, M. Hou, Z. Zhu, Z. Gu, *ACS Catal.* **2017**, *7*, 5316–5320; n) J. Zheng, W.-J. Cui, C. Zheng, S.-L. You, *J. Am. Chem. Soc.* **2016**, *138*, 5242–5245; o) T. Wesch, F. R. Leroux, F. Colobert, *Adv. Synth. Catal.* **2013**, *355*, 2139–2144; p) K. Yamaguchi, H. Kondo, J. Yamaguchi, K. Itami, *Chem. Sci.* **2013**, *4*, 3753–3757; q) K. Yamaguchi, J. Yamaguchi, A. Studer, K. Itami, *Chem. Sci.* **2012**, *3*, 2165–2169; r) F. Kakiuchi, P. Le Gendre, A. Yamada, H. Ohtaki, S. Murai, *Tetrahedron: Asymmetry* **2000**, *11*, 2647–2651.

[17] C.-X. Liu, W.-W. Zhang, S.-Y. Yin, Q. Gu, S.-L. You, *J. Am. Chem. Soc.* **2021**, *143*, 14025–14040.

[18] Y.-S. Jang, Ł. Woźniak, J. Pedroni, N. Cramer, *Angew. Chem. Int. Ed.* **2018**, *57*, 12901–12905; *Angew. Chem.* **2018**, *130*, 13083–13087.

[19] A. Romero-Arenas, V. Hornillos, J. Iglesias-Sigüenza, R. Fernandez, J. Lopez-Serrano, A. Ros, J. M. Lassaletta, *J. Am. Chem. Soc.* **2020**, *142*, 2628–2639.

[20] a) P. Hu, L. Kong, F. Wang, X. Zhu, X. Li, *Angew. Chem. Int. Ed.* **2021**, *60*, 20424–20429; *Angew. Chem.* **2021**, *133*, 20587–20592; b) F. Wang, J. Jing, Y. Zhao, X. Zhu, X.-P. Zhang, L. Zhao, P. Hu, W.-Q. Deng, X. Li, *Angew. Chem. Int. Ed.* **2021**, *60*, 16628–16633; *Angew. Chem.* **2021**, *133*, 16764–16769; c) J.

Wang, H. Chen, L. Kong, F. Wang, Y. Lan, X. Li, *ACS Catal.* **2021**, *11*, 9151–9158.
[21] Q. Dherbassy, J.-P. Djukic, J. Wencel-Delord, F. Colobert, *Angew. Chem. Int. Ed.* **2018**, *57*, 4668–4672; *Angew. Chem.* **2018**, *130*, 4758–4762.
[22] D. Liang, J.-R. Chen, L.-P. Tan, Z.-W. He, W.-J. Xiao, *J. Am. Chem. Soc.* **2022**, *144*, 6040–6049.
[23] a) Y.-J. Wu, G. Liao, B.-F. Shi, *Green Synth. Catal.* **2022**, *3*, 117–136; b) L. Sun, H. Chen, B. Liu, J. Chang, L. Kong, F. Wang, Y. Lan, X. Li, *Angew. Chem. Int. Ed.* **2021**, *60*, 8391–8395; *Angew. Chem.* **2021**, *133*, 8472–8476; c) O. Kitagawa, *Acc. Chem. Res.* **2021**, *54*, 719–730; d) T.-Z. Li, S.-J. Liu, W. Tan, F. Shi, *Chem. Eur. J.* **2020**, *26*, 15779–15792.
[24] For our previous works on enantioselective C–H activation, see: a) Y. Li, Y.-C. Liou, X. Chen, L. Ackermann, *Chem. Sci.* **2022**, *13*, 4088–4094; b) J. Frey, X. Hou, L. Ackermann, *Chem. Sci.* **2022**, *13*, 2729–2734; c) U. Dhawa, T. Wdowik, X. Hou, B. Yuan, J. C. A. Oliveira, L. Ackermann, *Chem. Sci.* **2021**, *12*, 14182–14188; d) U. Dhawa, C. Tian, T. Wdowik, J. C. A. Oliveira, J. Hao, L. Ackermann, *Angew. Chem. Int. Ed.* **2020**, *59*, 13451–13457; *Angew. Chem.* **2020**, *132*, 13553–13559; e) J. Loup, V. Müller, D. Ghorai, L. Ackermann, *Angew. Chem. Int. Ed.* **2019**, *58*, 1749–1753; *Angew. Chem.* **2019**, *131*, 1763–1767; f) J. Loup, D. Zell, J. C. A. Oliveira, H. Keil, D. Stalke, L. Ackermann, *Angew. Chem. Int. Ed.* **2017**, *56*, 14197–14201; *Angew. Chem.* **2017**, *129*, 14385–14389.
[25] Deposition number 2165781 (**33**) contains the supplementary crystallographic data for this paper. These data are provided free of charge by the joint Cambridge Crystallographic Data Centre and Fachinformationszentrum Karlsruhe Access Structures service.
[26] a) S. Feng, Y. Dong, S. L. Buchwald, *Angew. Chem. Int. Ed.* **2022**, *61*, e202206692; *Angew. Chem.* **2022**, *134*, e202206692; b) G. M. Schwarzwalder, C. D. Matier, G. C. Fu, *Angew. Chem. Int. Ed.* **2019**, *58*, 3571–3574; *Angew. Chem.* **2019**, *131*, 3609–3612; c) H. Yi, W. Mao, M. Oestreich, *Angew. Chem. Int. Ed.* **2019**, *58*, 3575–3578; *Angew. Chem.* **2019**, *131*, 3613–3616.
[27] For detailed information, please see the Supporting Information.

Manuscript received: August 25, 2022
Accepted manuscript online: September 15, 2022
Version of record online: October 20, 2022